



**HAL**  
open science

## Modeling in-stream biogeochemical processes at catchment scale: Coupling SWAT and RIVE models

Sarah Manteaux, Sabine Sauvage, René Samie, Céline Monteil, Josette Garnier, Vincent Thieu, Roxelane Cakir, José-Miguel Sánchez-Pérez

### ► To cite this version:

Sarah Manteaux, Sabine Sauvage, René Samie, Céline Monteil, Josette Garnier, et al.. Modeling in-stream biogeochemical processes at catchment scale: Coupling SWAT and RIVE models. *Environmental Modelling and Software*, 2023, 170, pp.105856. 10.1016/j.envsoft.2023.105856 . hal-04278645

**HAL Id: hal-04278645**

**<https://hal.science/hal-04278645>**

Submitted on 13 Nov 2023

**HAL** is a multi-disciplinary open access archive for the deposit and dissemination of scientific research documents, whether they are published or not. The documents may come from teaching and research institutions in France or abroad, or from public or private research centers.

L'archive ouverte pluridisciplinaire **HAL**, est destinée au dépôt et à la diffusion de documents scientifiques de niveau recherche, publiés ou non, émanant des établissements d'enseignement et de recherche français ou étrangers, des laboratoires publics ou privés.

# Modeling in-stream biogeochemical processes at catchment scale: coupling SWAT and RIVE models

Sarah Manteaux<sup>1</sup>, Sabine Sauvage<sup>2</sup>, René Samie<sup>1</sup>, Céline Monteil<sup>1</sup>, Josette Garnier<sup>3</sup>, Vincent Thieu<sup>3</sup>, Roxelane Cakir<sup>2</sup>, José-Miguel Sánchez-Pérez<sup>2</sup>

<sup>1</sup>Electricité de France – Laboratoire National d’Hydraulique et Environnement (LNHE), France (manteaux.sarah@orange.fr ; rene.samie@edf.fr ; celine-c.monteil@edf.fr)

<sup>2</sup>Laboratoire Ecologie Fonctionnelle et Environnement, Institut national polytechnique de Toulouse (INPT), CNRS, Université de Toulouse (UPS), France. (sabine.sauvage@univ-tlse3.fr ; jose-miguel.sanchez-perez@univ-tlse3.fr; cakir.roxelane@gmail.com)

<sup>3</sup>Sorbonne Université CNRS EPHE, UMR Metis 7619, 4 place Jussieu, 75005 Paris, France (josette.garnier@sorbonne-universite.fr; vincent.thieu@sorbonne-universite.fr)

## Highlights

- SWAT and RIVE models were coupled to enhance the modeling of in-stream biogeochemical processes in SWAT.
- An epilithic biofilm model was added to the coupled model.
- The coupled model was validated on a 89 km section of the Garonne watershed.
- Annual and seasonal interannual budgets for nutrients and organic matter were established.

## Abstract

The representation of biogeochemical in-stream processes is complex and requires the use of models to understand the factors controlling the transfer of contaminants at the scale of a watershed. The biogeochemical model RIVE was implemented into SWAT model and used, instead of current QUAL2E subroutine, to calculate biogeochemical in-stream processes. The coupled model was applied on a 89 km section of the Garonne watershed (France) downstream of Toulouse city, for the 2000-2010 period, with a daily time step. An epilithic biofilm equation was added to represent the algae communities in this river, dominated by drifted benthic diatoms. The model matches the observed data for the major water-quality variables. Nitrogen, phosphorus, silica, and organic suspended matter dominant processes were assessed. The goal of coupling RIVE to SWAT model was to improve the biogeochemical representation of the river’s in-stream ecological processes linked to C, N, P, Si elements and dissolved oxygen with minimal calibration.

## 33 **Keywords**

34 Water quality, model coupling, nutrient budget

## 35 **1. Introduction**

36 SWAT (Soil and Water Assessment Tool, Arnold et al., 1998) is one of the most applied  
37 hydro-agro-ecological models in the world, having been successfully implemented on a large  
38 variety of watersheds (Gassman et al., 2007, 2014; Krysanova and Arnold, 2008; Krysanova  
39 and White, 2015; Francesconi et al., 2016). This physically-based and semi-distributed agro-  
40 hydrological model was developed to predict the impacts of land use, land management  
41 practices and climate change on water quantity and quality. It simulates the transfer of  
42 biogenic elements from land to river at the watershed scale. The in-stream biogeochemical  
43 processes are simulated by a modified version of the QUAL2E model (Brown and Barnwell,  
44 1987), which takes into account the main transformations in nitrogen and phosphorus cycles  
45 only. Activation of this module is optional.

46

47 SWAT, with QUAL2E module activated, has demonstrated good performances in several  
48 studies, but mainly at monthly or annual scales (Gassman et al., 2007). However, other  
49 authors reported poor to moderate performances in simulating nutrient loads (Grunwald and  
50 Qi, 2006) or a need to refine the in-stream processes routine (White et al., 2014). The mass  
51 balance is not closed, the sedimentation and diffusion of nutrients from the streambed being  
52 disconnected. Migliaccio et al. (2007) found no enhancement in nutrient predictions when  
53 activating QUAL2E in SWAT instead of deactivating in-stream process simulation.  
54 [Moreover, the numerical method employed to solve the QUAL2E differential equations in](#)  
55 [SWAT can lead to instabilities and solution inconsistencies, particularly in reaches with](#)  
56 [extended residence times](#) (Woldegiorgis et al., 2017). Femeena et al. (2020) noted high daily  
57 fluctuations in dissolved oxygen simulations, whereas the ability to simulate dissolved oxygen  
58 concentrations was critical for water quality modeling, due to their influence on nitrogen and  
59 phosphorus cycles. Regarding phytoplankton, the module represents a total algae biomass,  
60 without considering the diverse physiological properties (growth, mortality, nutrients uptake  
61 rates) of different algal groups, nor the influence of silica on algal development. Furthermore,  
62 the module does not represent epilithic biofilm and is therefore not adequate for the systems  
63 where it is dominant (White et al., 2014). Regarding the nitrogen cycle, denitrification

64 remains unaccounted for, while benthic denitrification is a key process for nitrogen removal in  
65 streams (Xia et al., 2018). Finally, the QUAL2E module requires a systematic calibration,  
66 which is a challenging step for achieving robust water quality simulations (Gassman et al.,  
67 2007; Houser and Hauck, 2002).

68

69 To address SWAT in-stream biogeochemical processes representation gaps, external  
70 couplings were made, principally for better assessing nutrient transformations and algal  
71 growth in water bodies (coupling with WASP (Narasimhan et al., 2010) or CE-QUAL-W2  
72 (Debele et al., 2008)), or to simulate turbidity propagation in streams (coupling with CE-Qual-  
73 Riv1 (Noh et al., 2013)). In terms of internal couplings, Pyo et al., (2019) modified the  
74 QUAL2E algal module with CE-QUAL-W2 equations to simulate in-stream dynamics of  
75 three algal groups while Kim and Shin (2011) modified the QUAL2E module to simulate  
76 algal growth kinetics in detail to improve the accuracy of internal organic matter and bottle  
77 BOD5 simulation. These mentioned studies focused on one aspect of water quality (algae,  
78 organic matter). To our knowledge refinement was made on both phytoplankton and organic  
79 carbon simulations, as well as on processes occurring in the benthic zone, in order to  
80 comprehensively describe the fate of nitrogen and phosphorus in streams. Further, Femeena et  
81 al. (2020) integrated a new solute transport model developed based on OTIS (One-  
82 dimensional Transport with Inflow and Storage) to account for advection, dispersion, transient  
83 storage exchange and calculate at sub-daily scale and smaller segments. However, the  
84 computational time was 60 times longer, so they recommended to use the model only for  
85 small time period simulations. In ESWAT (Van Griensven and Bauwens, 2003), the riverbed  
86 mass balance **was closed** and the numerical scheme was modified with the use of an hourly  
87 time step. The mixing of the inflow occurred after applying concentration transformation to  
88 the channel's initial concentration at the beginning of the time step. Nonetheless, instabilities  
89 were still observed, as noted by **these authors**. The recent quasi-analytical solution proposed  
90 by Woldegiorgis et al. (2017) for QUAL2E in SWAT has provided stable and consistent  
91 solutions **in our own modeling**.

92

93 RIVE model is a mechanistic model that describes in-stream ecological and biogeochemical  
94 processes. It was developed to understand the dynamics of nutrients, the trophic chain in the  
95 river systems, and the development of three types of algae within rivers. It was implemented  
96 in several models: Riverstrahler (Billen et al., 1994; Garnier et al., 1995), ProSe (Even et al.,  
97 1998), pyNuts-Riverstrahler (Thieu et al., 2022), and QUAL-NET (Minaudo et al., 2018). It

98 was developed and mainly applied on the Seine River, and successfully applied for a variety  
99 of watersheds such as Somme, Scheldt (Thieu et al., 2009), Danube (Garnier et al., 2002),  
100 Loire (Garnier et al., 2018a), Red River (Le et al., 2010), Kalix (Sferratore et al., 2008) and on  
101 the Garonne major tributary, the Lot River (Garnier et al., 2018b). RIVE model considers the  
102 physiology of algal developments and simulates biogeochemical cycles of carbon, nitrogen,  
103 phosphorus and silica along hydrographic networks, including interactions between the water  
104 column and the benthic zone. RIVE's equations and parameters were determined based on  
105 experiments and directly linked to easily measurable environmental variables. RIVE does not  
106 require calibration, although the narrow range of parameter determination can be possibly  
107 explored in case of strong disagreement with observed variables . Currently, RIVE model is  
108 undergoing revision and unification by the Metis Lab developers' team and will soon be made  
109 accessible to the scientific community through a collaborative platform at  
110 (<https://gitlab.in2p3.fr/rive>).

111

112 RIVE model was integrated into SWAT, and a section of the Garonne watershed in France  
113 was selected for model testing and validation. This choice was based on the availability of  
114 numerous studies and measurements, providing all the necessary data for analysis. The  
115 section, extending from Toulouse to the Malause reservoir, receives the urban effluents of  
116 Toulouse city and is therefore an appropriate site to evaluate their impact on water quality. As  
117 the Garonne River is a system dominated by epilithic biofilm (Améziane et al., 2003), an  
118 epilithic biofilm module was also added.

119

120 The objectives of this study were (i) to model detailed in-stream ecological processes by  
121 integrating and validating RIVE model into SWAT, (ii) to assess the dynamic of the dominant  
122 nutrient cycles and particulate organic matter in a section of the Garonne River.

## 123 **2. Material and methods**

### 124 **2.1.1. Models overview**

#### 125 **SWAT model**

126 SWAT calculations are conducted on a daily time step, and the outputs can be generated on a  
127 daily, monthly, or yearly basis. The watershed is spatially discretized into sub-basins, which  
128 are divided into hydrological response units (HRU), a unique combination of slope, soil type  
129 and land use. Water, sediment, and nutrients are calculated at the HRU scale, aggregated at

130 the sub-basin level, and routed through the hydrographic network to the outlet. The variables  
 131 and processes in SWAT land phase are summarized in Table 1. Carbon cycle is only  
 132 calculated in the land phase. In the streams, the QUAL2E module includes eight variables:  
 133 algae (as chlorophyll a), dissolved oxygen, carbonaceous oxygen demand, organic nitrogen,  
 134 ammonium, nitrite, nitrate, and soluble and organic phosphorus. Further details can be found  
 135 in Neitsch et al. (2011).

136

137 Table 1: SWAT land processes

<b>Variables</b>	<b>Land processes</b>	<b>Transfers to reach</b>
Water	Evapotranspiration, infiltration, runoff, plant uptake, percolation, lateral flow, groundwater flow	Runoff, lateral flow, groundwater flow
Nitrogen (organic, nitrate, nitrite, ammonia)	Plant uptake, nitrification, denitrification, ammonia volatilization, atmospheric deposition and fixation, mineralization, immobilization, nitrate leaching, nitrate loss in shallow aquifer	Nitrate in runoff, lateral flow and groundwater flow, organic nitrogen in runoff
Phosphorus (organic, mineral)	Mineralization, immobilization, sorption, leaching	Organic and soluble P in runoff, mineral P attached to sediment in runoff, soluble P in groundwater flow
Carbon	Static content or decomposition, humification	
Sediment	Water erosion	Total suspended sediment load

138

## 139 **RIVE model**

140 RIVE model performs calculations using time steps ranging from six minutes to one hour. In  
 141 the version used, 35 state variables are defined: nutrients (nitrate, ammonium, nitrite, total  
 142 inorganic phosphorus, orthophosphates, dissolved and biogenic silica), suspended matter,  
 143 biological compartments (three kind of phytoplankton, two of zooplankton, two of  
 144 heterotrophic bacteria, two of nitrifying bacteria, two of fecal bacteria), seven compartments  
 145 of non-living organic matter (particulate and dissolved, with three classes of biodegradability  
 146 each, and small organic substrate directly uptaken), dissolved oxygen and nitrous oxide for  
 147 the water column; and for the benthos, three compartments of organic matter (classes of  
 148 biodegradability) and deposited matter, silica, inorganic phosphorus and fecal bacteria. The  
 149 model accounts for the filtration by lamellibranchs. Their impact on phytoplankton dynamics  
 150 is represented as a constraint, their complex life cycle is not modeled. The processes  
 151 represented within the model are summarized in Table 2. Benthic nutrient fluxes are  
 152 calculated according to the new simplified algorithm (Billen et al., 2015).

153

154 *Table 2: Processes represented in RIVE model, based on Garnier et al. (2002), Ruelland et al. (2007a)*

<b>Variables</b>	<b>Processes</b>
Suspended and deposited sediment	Sedimentation, erosion

Phytoplankton	Photosynthesis, growth, respiration, lysis, sedimentation
Zooplankton	Grazing, growth, respiration, mortality
Heterotrophic bacteria	Organic matter degradation, growth, mortality, sedimentation
Non-living organic matter	Hydrolysis, sedimentation, compaction, erosion, phytoplankton excretion
Dissolved oxygen	Photosynthesis, respiration, nitrification, benthic consumption
Nitrogen	Phytoplankton and heterotrophic bacteria uptake, ammonification, nitrification, water column and benthic denitrification and nitrous oxide production, benthic remineralization, nitrous oxide ventilation
Nitrifying bacteria	Growth, mortality, sedimentation
Phosphorus	Phytoplankton uptake, adsorption and desorption, benthic remineralization, zooplankton and heterotrophic bacteria mineralization, erosion, sedimentation, compaction
Silica	Diatoms uptake, dissolution, water-sediment interface flux, sedimentation, erosion, compaction
Fecal bacteria	Mortality, sedimentation

---

155

## 156 **Epilithic biofilm model**

157 The Boulêtreau et al. (2006)'s epilithic biofilm model added was adapted from Uehlinger et  
158 al. (1996) and precisely developed on the Garonne watershed. We opted for the three-  
159 parameter model, which accounts for net biomass growth restricted by biomass thickness and  
160 a detachment term that varies in proportion to the mean daily discharge  $Q$ . The detachment  
161 coefficient ( $cdet$ ) was set to  $0.0016 \text{ s m}^{-3} \text{ d}^{-1}$ , the maximum specific growth rate ( $\mu_{max}$ ) to  
162  $7.84 \text{ d}^{-1}$ , and the inverse half-saturation constant ( $k_{inv,B}$ ) to  $3.8 \text{ g ash-free dry mass [AFDM]}^{-1}$   
163  $\text{m}^2$ .  $B$  is the epilithic biomass ( $\text{g AFDM m}^{-2}$ ) and  $B0$  the minimal biomass ( $\text{g AFDM m}^{-2}$ ).

$$164 \quad \frac{dB}{dt} = \mu_{max} \times B \times \frac{1}{1+k_{inv,B} \times B} - cdet \times Q \times (B - B0) \quad (3)$$

165 The detachment term gives the drifted biofilm biomass. To convert the detached biomass from  
166  $\text{gAFDM.m}^{-2}$  to  $\text{mgC.l}^{-1}$ , we utilized SWAT-estimated reach length and width, with the latter  
167 adjusted due to overestimation. We applied a coefficient of 0.4 corresponding to the surface of  
168 riffles in this section of the Garonne according to Simeoni-Sauvage (1999), where biofilm  
169 develops. The autotrophic index (i.e., ratio AFDM/chlorophyll a) was set to 100, mean value  
170 calculated on Garonne epilithic biofilm data. RIVE model diatoms equations and parameters  
171 were applied to drifted biofilm, as epilithic algal communities are dominated by this algal  
172 group (Eulin and Le Cohu, 1998).

173 Nitrate, nitrite, and ammonia exchanges between the water column and the biofilm were set  
174 according to Teissier et al. (2007) daily budgets determined on the Garonne in its middle  
175 course, with a threshold of  $23 \text{ g AFDM m}^{-2}$  between photoautotrophy and heterotrophy.

## 176 **Coupled SWAT-RIVE model**

177 We used the version SWAT2012 VER 2016/Rev 664. The coupling with RIVE model is  
178 internal. A subroutine containing RIVE equations was integrated into SWAT. This subroutine

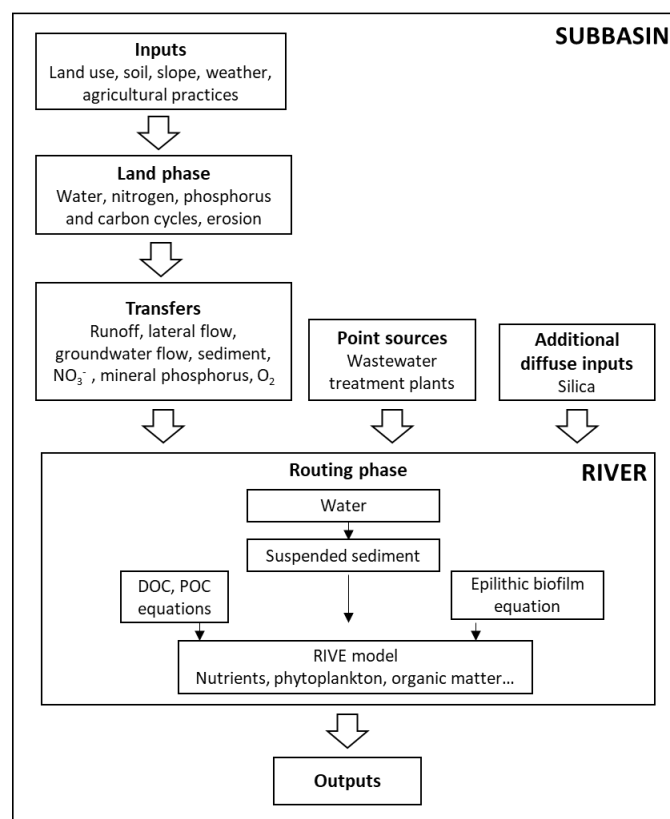
179 is called instead of QUAL2E when the parameter IWQ (in .bsn file) is set to 3 (IWQ 0 = do  
180 not use QUAL2E, 1 = use QUAL2E, 3 = use RIVE). The historical version of the RIVE code  
181 ([https://gitlab.in2p3.fr/rive/original\\_vb\\_code](https://gitlab.in2p3.fr/rive/original_vb_code)), initially in Visual Basic, was used and  
182 transcribed into Fortran 90 language to be integrated into SWAT model. The coupled model  
183 space scale (river reach) and time scale (daily) are the same as SWAT. The RIVE module has  
184 been implemented following the structure of the QUAL2E module included in SWAT, with a  
185 small modification. The module is called by reach (as defined in SWAT, one per sub-basin)  
186 and once a day, but we added an hourly loop to calculate variations and update concentrations  
187 every hour during the travel time within the reach. This method prevents instabilities that  
188 could occur in reaches with high residence times.

### 189 *SWAT and RIVE connection*

190 The land phase is simulated by SWAT, which calculates water fluxes, nutrients cycles and  
191 suspended sediment erosion, subsequently determining the resulting loads to the reach (Figure  
192 1). Water fluxes are simulated by the SWAT subroutine, while nutrient transformations are  
193 handled by the RIVE subroutine. Both models initially calculate processes related to  
194 suspended sediments. SWAT computes the deposition and degradation of total suspended  
195 sediments (TSS) in the channel while RIVE computes total suspended sediments deposition  
196 and degradation, along with additional processes for organic suspended sediments and  
197 phosphates adsorption-desorption (see Table 2). To avoid double-counting of TSS deposition  
198 and degradation, the choice was made to keep the in-stream sediment subroutine of SWAT.  
199 Organic suspended sediments processes were simulated by RIVE. Silica and organic carbon  
200 diffuse inputs are required by RIVE but not calculated by SWAT. Consequently, dissolved  
201 silica diffuse inputs were determined with lithology, giving a constant concentration in  
202 surface runoff and groundwater flow by rock types (Meybeck, 1986), values used for the  
203 application of Riverstrahler on the Lot River, Garonne tributary (Garnier et al. (2018b). For  
204 biogenic silica, an average content of  $4.9 \text{ mgSi.gTSS}^{-1}$  was applied. This value was estimated  
205 by Sferratore et al. (2006) in the Seine basin from measurements of silica in winter in TSS and  
206 in soils. Organic carbon diffuse inputs were not directly computed: organic carbon  
207 concentrations at the beginning of each day were estimated in every reach from equations  
208 linking dissolved organic carbon to discharge and particulate organic carbon to suspended  
209 sediments (see Table 3). DOC parameters were set to the mean values of the parameters  
210 determined on 50 stations of the Garonne watershed. POC parameters were calculated on the  
211 Save tributary, due to limited available data for the Garonne. The simulated DOC and POC  
212 concentrations were validated with observations at Verdun-sur-Garonne (see Figure 2), . Once



213 the quantity of COD and COP is determined, RIVE requires their distribution among the  
 214 biodegradability classes: rapid (5 days), medium to slow (45 days), refractory. For DOC, the  
 215 values determined for the Seine River were applied i.e., 9, 21, and 70% for rapidly  
 216 biodegradable, slowly, and refractory respectively (Vilmin et al., 2015). For COP, a similar  
 217 distribution was based on the percentage curve of POC in relation to TSS for the Garonne  
 218 River. Specifically, when the TSS concentration is less than  $5 \text{ mg.l}^{-1}$ , COP consists solely of  
 219 rapidly biodegradable COP, primarily from phytoplankton for this watercourse; for TSS  
 220 concentrations between 5 and  $20 \text{ mg.l}^{-1}$ , the calculated COP is considered to be slowly  
 221 biodegradable COP, and for TSS concentrations greater than  $20 \text{ mg.l}^{-1}$ , it is categorized as  
 222 refractory COP.



223

224

Figure 1: Structure of the SWAT-RIVE model

225 Table 3 : Methodology applied for RIVE model inputs

Input type	Variable	Method
Climate and hydrology	Discharge, Flow velocity, Depth, Water temperature	Calculated daily by SWAT
Diffuse emissions	Suspended sediment, Nitrate, Mineral phosphorus, Oxygen	Calculated daily by SWAT
	Dissolved silica	Mean concentrations in surface runoff and groundwater flow according to lithology (3 mgSi.l <sup>-1</sup> for metamorphic rocks, 5 mgSi.l <sup>-1</sup> for sedimentary rocks (Garnier et al.(2018b), according to Meybeck (1986))
	Biogenic silica	A mean content of 4.9 mgSi.g <sup>-1</sup> of suspended matter (observations in the Seine catchments by Sferratore et al., (2006))
	Dissolved organic carbon (DOC)	$[DOC] = \frac{\alpha \cdot Q}{\beta + Q}$ (Fabre et al., 2020, 2019) With [DOC] DOC concentration (mg.l <sup>-1</sup> ), Q discharge (mm), $\alpha$ and $\beta$ parameters (set to 3.3 and 0.15 respectively)
Point sources	Particulate organic carbon (POC)	$\%POC = \frac{d}{TSS-a} + b$ (Boithias et al.,2014; Fabre et al.,2019) With %POC the percentage of POC in the total suspended sediments (TSS), d, a and b parameters (set to 9.40, 5 and 2.1 respectively (Boithias et al.,2014))
	Discharge, Suspended sediment, Nitrate, Ammonium, Nitrite, Mineral phosphorus, Oxygen	Already in SWAT wastewater treatment plants input files. Loads from Agence de l'eau (http://adour-garonne.eaufrance.fr/), except O <sub>2</sub> : fluxes estimated from capacity and treatment type, according to the methodology described for Seneque-Rivertrahler model in Ruelland et al. (2007b), Seneque 3.6 values
	Nitrifying and heterotrophic bacteria, silica, fecal bacteria, nitrous oxide	Addition to the wastewater treatment plants input files and to SWAT code. Fluxes estimated from capacity and treatment type, according to the methodology described for Seneque-Rivertrahler model in Ruelland et al. (2007b), Seneque 3.6 values

226

227 *Initialization*

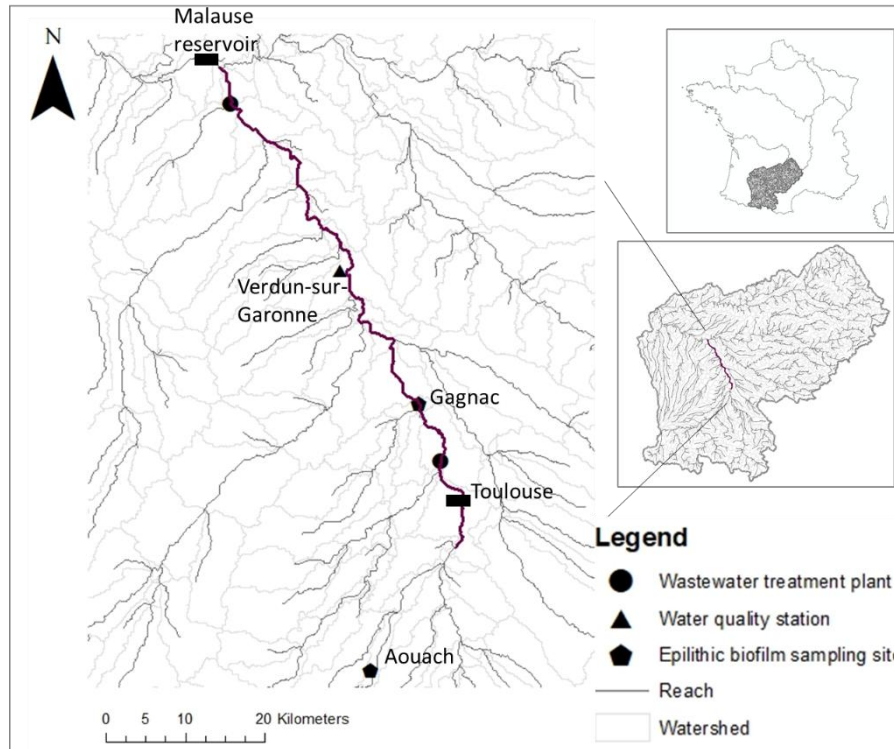
228 Initial values for water column variables were not assigned. Loads come from lands and point  
229 sources and a warm-up period determined the initial concentrations. The benthos variables  
230 were initialized homogeneously in each reach, using default parameters provided with the  
231 historical RIVE code ([https://gitlab.in2p3.fr/rive/original\\_vb\\_code](https://gitlab.in2p3.fr/rive/original_vb_code)). The model is supposed to  
232 have reached an equilibrium at the end of the warm-up period.

## 233 2.1.6. Study site: the Garonne River in its middle 234 course

### 235 2.2.1 Study area

236 The coupled model was validated on a section of the large Garonne River, of 600 km long  
237 with a watershed area of 60,000 km<sup>2</sup>, located in southwestern France. The study site is the  
238 section from Toulouse (one million inhabitants) to Malause reservoir, halfway between the  
239 source and the estuary (Figure 2). The section is 89 km long, seventh order, with a mean  
240 annual discharge of 200 m<sup>3</sup> s<sup>-1</sup>, a mean water velocity 0.5 m s<sup>-1</sup>, a shallow depth (mean 1 m)

241 and a wide bed (100 m) (Améziane et al., 2003). Garonne River middle course is  
242 characterized by two high-flow periods, with hydrological maxima in February and May, and  
243 a low-flow period in summer.  
244



245  
246

Figure 2: The Garonne River section studied (in bold)

## 247 2.2.2 Input data and calibration/validation

248 The SWAT project used in this study has been set up, calibrated (for the period of 2000-  
249 2010), and validated (for the period of 1990-1999) for the study of hydrological and nitrate  
250 processes in the whole Garonne watershed by Cakir et al. (2020). Comprehensive details  
251 regarding data requirements for this SWAT project can be found in Cakir et al. (2020). The  
252 calibration of diffuse nitrate inputs was carried out by Cakir et al. (2020) based on crop yields.  
253 SWAT-RIVE validation was carried out for the period from 2000 to 2010, with a warm-up  
254 period of three years.. Parameters from the original model were used without change, except  
255 for the particulate organic carbon sedimentation sinking rate, which was adjusted to 0.006  
256  $\text{m}\cdot\text{h}^{-1}$  (instead of xxxx) in accordance with the composition of particulate organic matter in the  
257 Garonne watershed. The RIVE subroutine was activated on the whole watershed, providing  
258 upstream boundary conditions to the 89 km river section studied. The data used for validation  
259 are listed in Table 4.

260

261 *Table 4: Observation data sources*

Data type	Data sources	Resolution		Description
		Spatial	Temporal	
Discharge	<a href="https://hydro.eaufrance.fr/">https://hydro.eaufrance.fr/</a>	Verdun-sur-Garonne	Daily (2000–2010)	River daily discharge at 1 sampling site
Nutrients, oxygen, chlorophyll a, DOC, POC, suspended sediments	Agence de l'eau ( <a href="http://adour-garonne.eaufrance.fr/">http://adour-garonne.eaufrance.fr/</a> )	Verdun-sur-Garonne gauging station	Punctual (2000–2010)	Concentrations at 1 sampling site, once a month
POC, suspended sediments	(Oeurng et al., 2011)	Save tributary	Daily (2008-2009)	Concentrations at 1 sampling site, once a day
Epilithic biofilm	(Boulêtreau et al., 2006)	Aouach and Gagnac sites	Punctual	2 sampling sites, 1 campaign (2001-2002)

262

263 Additional input data required by RIVE concerned silica and carbon diffuse fluxes, as well as  
 264 supplementary point sources loads (see Table 3). Nineteen additional wastewater treatment  
 265 plant point sources were added to the original SWAT project due to [the significant role of](#)  
 266 [wastewater treatment plant effluents in seeding heterotrophic bacteria \(Garnier et al. 1992\)](#)  
 267 [and nitrifying bacteria\(Brion and Billen, 2000\).](#)

268 **2.2.3 Model performance**

269 Indices were calculated to validate the model: the Nash-Sutcliffe efficiency (NSE) index, the  
 270 coefficient of determination ( $R^2$ ), and the percent of bias (PBIAS), as described in Moriasi et  
 271 al. (2015). For water quality modeling, the values considered satisfactory for nitrogen are:  
 272  $NSE > 0.35$ ,  $R^2 > 0.3$  and  $PBIAS < 30$ , and good:  $NSE > 0.5$ ,  $R^2 > 0.6$  and  $PBIAS < 20$   
 273 (Moriasi et al., 2015). For phosphorus, the same ranges apply to NSE and PBIAS, and the  
 274 simulation is considered satisfactory if  $R^2 > 0.4$  and good if  $R^2 > 0.65$ . The root mean square  
 275 error (RMSE) and the Kling-Gupta efficiency criterion (KGE) (modified version, Kling et al.,  
 276 2012) were also computed for validation purposes.

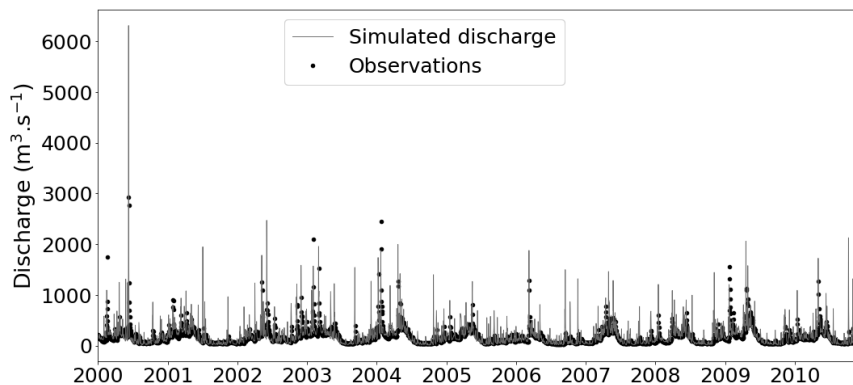
277

## 278 3. Results and discussion

### 279 3.1. Model results and validation

#### 280 3.1.1 Hydrology

281 The hydrology simulation on the whole watershed showed satisfactory results, with the  
282 simulation reproducing well observed trends (Figure 3, see Cakir et al., 2020 for details on  
283 calibration and validation results).



284

285 *Figure 3: Observed and simulated discharges at Verdun-sur-Garonne on a daily time scale for 2000–2010*

#### 286 3.1.2 Nutrients and oxygen

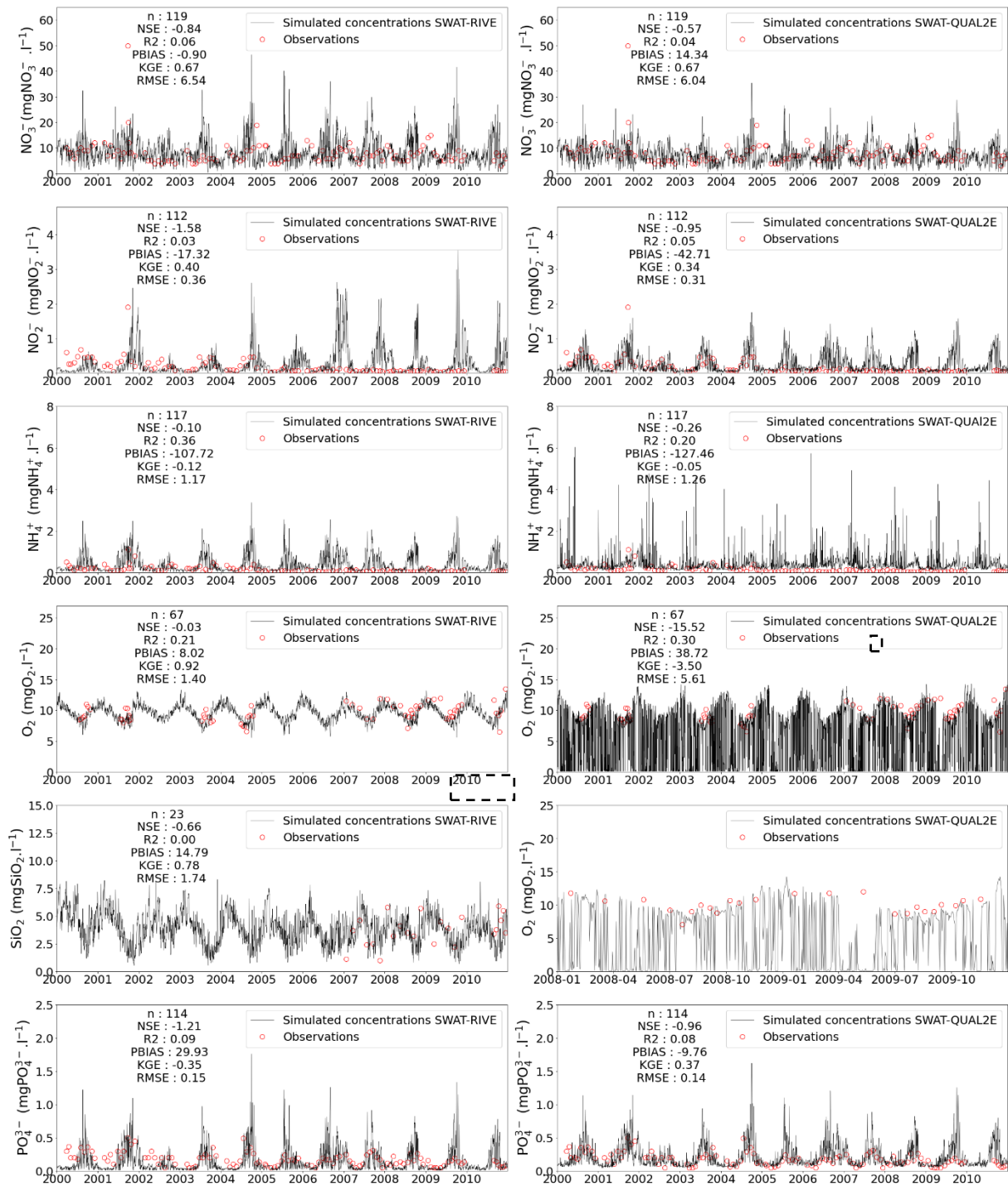
287 The concentrations obtained with SWAT-RIVE and SWAT-QUAL2E modules were  
288 compared to available observations in the Toulouse-Malause section, specifically at the  
289 Verdun-sur-Garonne station, which is located approximately in the middle of the section  
290 (Figure 4). Nitrate simulation results using RIVE were close to the concentrations obtained  
291 with SWAT with QUAL2E subroutine, but with higher peak concentrations. Nitrite and  
292 ammonia were overestimated in both models, especially after 2005. Dissolved silica  
293 concentrations were simulated with SWAT-RIVE in accordance with the observations range,  
294 although there were limited observations available, only covering the period from 2007 to  
295 2010. Orthophosphates concentrations simulation showed a similar trend in both models.

296 SWAT-RIVE and SWAT-QUAL2E performance indices were mostly below Moriasi et al.  
297 (2015) standards, probably because observations were measured only once a month or less.  
298 Nevertheless, nitrate simulation KGE was 0.67 for both models, and PBIAS was satisfactory  
299 for SWAT-QUAL2E (14.3) and very good for SWAT-RIVE (-0.9). Compared to SWAT-  
300 QUALE, SWAT-RIVE PBIAS performances were better for the nitrogen forms. For

301 orthophosphates, PBIAS performances were lower for SWAT-RIVE, although the  
302 concentrations simulated with the two models were close. Simulated nutrients concentrations  
303 were in the range of the observations and the seasonal and interannual variations were  
304 reproduced.

305 The oxygen simulation with SWAT-RIVE reproduced the seasonal variations observed and  
306 was improved compared to SWAT-QUAL2E, the latter simulating dissolved oxygen drops  
307 down to  $0.1 \text{ mgO}_2\cdot\text{l}^{-1}$ . The simulations extremely low here for oxygen concentrations are  
308 correlated with high CBOD concentrations. These instabilities result from the numerical  
309 solving method used in SWAT-QUAL2E. Calibration may address this limitation. Similar  
310 extreme low oxygen concentration values simulated with SWAT-QUAL2E were reported by  
311 Femeena et al. (2020), and the simulation of dissolved oxygen was improved by modifying  
312 dissolved oxygen and CBOD equations, as well as solute dynamics. Comparisons between  
313 SWAT-RIVE and SWAT-QUAL2E confirmed the interest in using a biogeochemical model  
314 like RIVE, with more processes involved, without calibration or only limited parameter  
315 adjustments.

316



317

318

319

Figure 4: Nutrients and oxygen concentrations simulated daily with SWAT-RIVE model (left) and SWAT-QUAL2E model (right) and observed, at Verdun-sur-Garonne for 2000-2010.

320

### 321 3.1.3 Epilithic biofilm and chlorophyll a

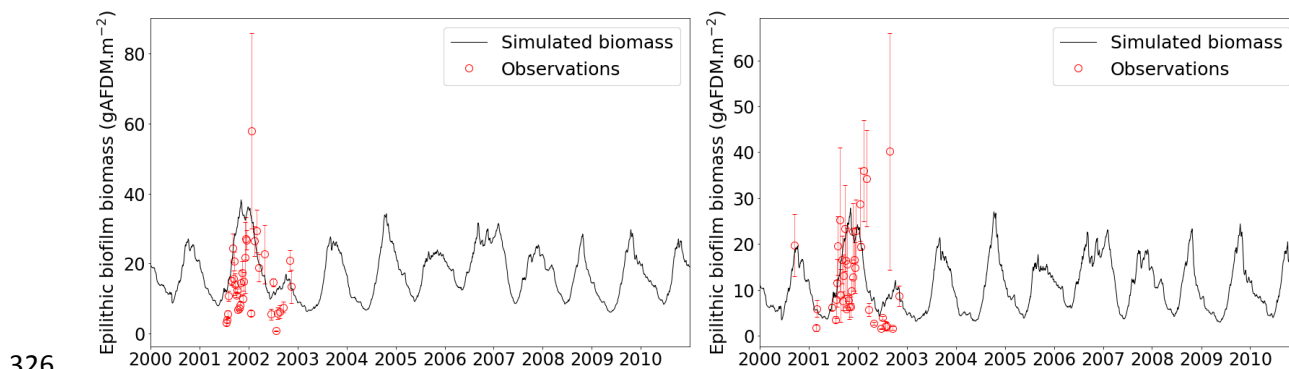
322

Epilithic biofilm observations have been limited to two sites: the Aouach site upstream of

323

Toulouse, and the Gagnac site downstream of Toulouse. The attached biofilm biomass

324 simulated by the model reproduced the trends observed on the two sites during the campaign  
325 (2001-2002) (Boulêtreau et al., 2006) (Figure 5).

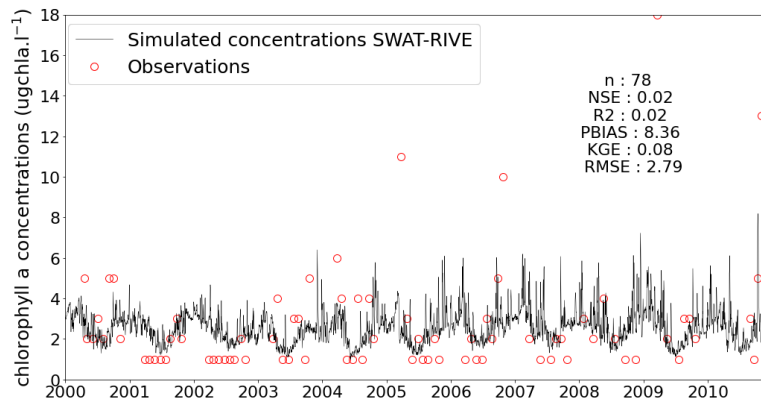


326  
327 *Figure 5: Attached epilithic biofilm biomass simulated by the model and measured at Aouach (upstream of*  
328 *Toulouse) (left) and Gagnac (downstream of Toulouse) (right)*

329 Total chlorophyll a simulated and measured were compared (Figure 6). Simulated chlorophyll  
330 a concentrations varies between 1 to 8  $\mu\text{g chla.l}^{-1}$  and observations mostly ranged from 1  
331 (quantification limit) to 6  $\mu\text{g chla.l}^{-1}$ , with four values above 10  $\mu\text{g chla.l}^{-1}$ . Chlorophyll a  
332 would mainly originate from detached benthic diatoms (from 94.9 to 98.9 %, see Table 5)  
333 while phytoplankton production is low, in line with previous studies on the Garonne River.  
334 Tekwani et al. (2013) indeed reported that benthic diatoms accounted for 99% of the water  
335 column community in a sampling site 36 km upstream of Toulouse. The percentages of  
336 benthic diatoms in suspended algae sampled by Amézière et al. (2003) were lower, between 6  
337 to 52% for Toulouse and Verdun sites, but the conclusions were that the drift of benthic  
338 diatoms constituted the major part of chlorophyll a in the Garonne, as high turbulence and  
339 short residence time were not favorable to phytoplankton development. Phytoplankton  
340 development was observed in tributaries (Tarn, Ariège) or in upstream reservoirs. The  
341 development of phytoplankton in reservoirs was not considered here in our modeling  
342 approach. Therefore, the observed increase in phytoplankton biomasses cannot be represented  
343 by this coupled model at this time. Modeling reservoirs using SWAT-RIVE could be a  
344 prospect of improvement, especially since reservoirs influence biogeochemical cycles and can  
345 act as sink of N, P and Si, impacting downstream concentrations (Garnier et al., 2000;  
346 Maavara et al., 2014; Sow et al., 2016; Yan et al., 2021).

347





348

349 *Figure 6: Simulated and observed concentrations of chlorophyll a at Verdun-sur-Garonne for 2000-2010.*

350 *Table 5: Phytoplankton species distribution simulated, monthly interannual mean percentage, at Verdun-*  
 351 *sur-Garonne for 2000-2010.*

Phytoplankton species	Jan	Feb	Mar	Apr	May	Jun	Jul	Aug	Sep	Oct	Nov	Dec
Chlorophyceae (%)	0.58	0.58	0.63	0.79	1.00	1.62	4.15	4.02	2.33	1.08	0.65	0.63
Cyanobacteria (%)	0.10	0.09	0.10	0.11	0.13	0.16	0.17	0.15	0.12	0.10	0.10	0.10
Diatoms (%)	0.41	0.44	0.51	0.67	0.85	0.95	0.82	0.67	0.48	0.42	0.45	0.43
Drifted benthic diatoms (%)	98.91	98.89	98.76	98.42	98.02	97.27	94.86	95.17	97.07	98.39	98.80	98.83
Total phytoplankton ( $\mu\text{g chla.l}^{-1}$ )	3.09	3.17	3.11	2.70	2.32	1.97	1.76	2.01	2.50	2.91	2.95	2.94

352

## 353 **3.2. Nutrients and organic suspended matter budgets**

354 The coupled model was used to explore the main processes occurring in the drainage network.

### 355 **3.2.1 Nitrogen budget**

356 On the studied section of 89 km downstream of Toulouse, nitrate would mainly originate from  
 357 upstream (64%), point sources along the section (25%), and tributaries (11%); nitrite  
 358 distributed from upstream (48%) and tributaries (44%) and ammonia from point sources  
 359 (77%) and upstream (22%) (Figure 7).

360 Nitrate and ammonia point source inputs were high, 25% and 77% of the entries respectively,  
 361 as the section included Toulouse wastewater treatment plants discharges. In 1992-1993  
 362 Muylaert et al. (2009) measured a doubling in dissolved inorganic nitrogen between the  
 363 upstream and downstream of Toulouse, which was attributed to intensive agriculture and  
 364 waste discharges. A decrease in ammonia and nitrite measured concentrations was observed  
 365 from the year 2005. This decline coincided with improvements in nitrogen and phosphorus  
 366 treatments at Toulouse's main wastewater treatment plant (WWTP Toulouse Ginestous). This

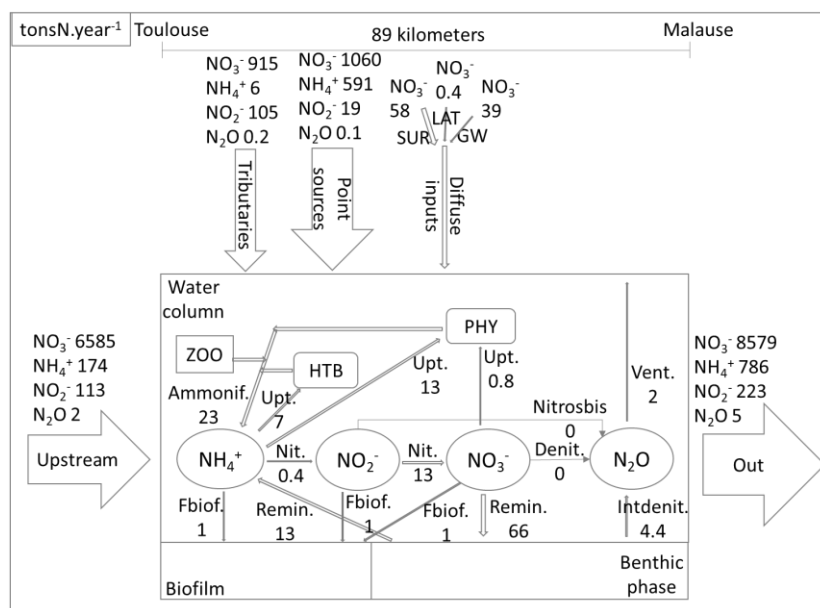
367 decrease was not simulated, as a constant WWTP nutrient discharge was implemented in the  
368 model. To account for it, another SWAT point source methodology could be applied, such as  
369 yearly records.

370 Diffuse nitrate inputs were calibrated by Cakir et al. (2020) based on crop yields. Direct  
371 diffuse inputs from the lands surrounding the Garonne were dominated by runoff and  
372 groundwater loads. This section of the Garonne River contains a large cultivated alluvial  
373 floodplain, where groundwater nitrate concentrations can exceed  $50 \text{ mgNO}_3^- \cdot \text{l}^{-1}$  but are much  
374 lower in the riparian zone due to plant uptake and denitrification (Pinay et al., 1998, Sánchez-  
375 Pérez et al., 2003). In particular, river water recharge dilutes nitrate concentrations and  
376 provides dissolved organic carbon promoting denitrification (Sánchez-Pérez et al., 2003).  
377 SWAT does not simulate river to aquifer fluxes and denitrification at the surface water-  
378 groundwater interface. To model these processes in SWAT, Sun et al. (2016) developed  
379 SWAT-LUD and estimated a reduction of 79% of nitrate entering this Garonne floodplain  
380 aquifers (Sun et al., 2018). In the SWAT version used in this study, nitrate biological and  
381 chemical removal in aquifers is estimated using a half-life parameter. We calibrated this  
382 parameter to account for nitrate reduction at the surface water-groundwater interface. With the  
383 calibration of this parameter for 2 years, determined by fitting simulated and observed data in  
384 low flow period, nitrate removal in aquifers was estimated at 65% of incoming flux into the  
385 aquifers in this section of the Garonne watershed.

386 The in-stream processes led to the consumption of  $55 \text{ tonsN} \cdot \text{year}^{-1}$  of nitrate present in the  
387 water column which represented 0.6% of the inputs, mainly lost at the water-benthos  
388 interface. In absolute values and percentages of the inputs, nitrate was more removed in  
389 autumn (Table 6). Retention in sediments and riparian zones is also a dominant process for  
390 nitrogen for studies using Seneque-Riverstrahler (on the Seine, the Somme, and the Scheldt  
391 rivers: Thieu et al., 2009: the Red River: Le et al., 2010: the Seine, Haut Loir and Red Rivers:  
392 Billen et al., 2018). The mean benthic denitrification rate estimated here was  $0.34 \text{ mgN m}^{-2} \text{ h}^{-1}$ ,  
393 which is low compared to the estimations on the Seine watershed ( $15 \text{ mgN m}^{-2} \text{ h}^{-1}$ : Billen et  
394 al., 2007, obtained with bell jars). Benthic denitrification produced  $4.4 \text{ tonsN} \cdot \text{year}^{-1}$  of nitrous  
395 oxide, with 39% produced in autumn. There was no water column denitrification, in  
396 accordance with our expectations, as there were no low-oxygen conditions. There was a  
397 production of  $15 \text{ tonsN} \cdot \text{year}^{-1}$  of ammonia (1.9% of the inputs), mainly by ammonification.  
398 Phytoplankton uptook ammonia ( $15.5 \text{ tonsN} \cdot \text{year}^{-1}$ ) preferentially to nitrate ( $0.8 \text{ tonsN} \cdot \text{year}^{-1}$ ).  
399 The N exchanges between the water column and the biofilm were low (around  $1 \text{ tonN} \cdot \text{year}^{-1}$

400 per N form consumed ( $\text{NO}_3^-$ ,  $\text{NO}_2^-$  and  $\text{NH}_4^+$ ), due to an equilibrium between uptake in the  
 401 light (photosynthesis) and release in the dark (respiration) (Teissier et al., 2007).

402 13 tonsN.year<sup>-1</sup> of nitrite was converted into nitrate (9% of the inputs) while only 0.5  
 403 tonN.year<sup>-1</sup> of ammonia was transformed into nitrites. Nitrification rate calculated can be  
 404 underestimated. Brion and Billen (2000) showed that wastewater treatment plants discharges  
 405 can represent an important seeding of nitrifying bacteria, controlling nitrification rates.  
 406 Additional point sources were added to the project to allow this seeding, but they do not  
 407 represent all urban effluents, only the 26 biggest wastewater treatment plants were  
 408 implemented.



409

410 *Figure 7: N budget on Toulouse-Malause section estimated with SWAT-RIVE model, interannual averages,*  
 411 *in tons of N per year, during the period 2000 to 2010.  $\text{NH}_4^+$ : ammonia,  $\text{NO}_3^-$ : nitrate,  $\text{NO}_2^-$ : nitrite,  $\text{N}_2\text{O}$ :*  
 412 *nitrous oxide, PHY: phytoplankton, HTB: heterotrophic bacteria, ZOO: zooplankton, Upt.: phytoplankton*  
 413 *or heterotrophic bacteria uptake, Denit: water column denitrification, Nitrosbis:  $\text{N}_2\text{O}$  production by*  
 414 *nitrification, Intdenit.: benthic denitrification, Nit.: nitrification,  $\text{NO}_3^-$ bent : nitrate flux across the water-*  
 415 *sediment interface, Amonnif: ammonification by heterotrophic bacteria, zooplankton, and lamellibranch,*  
 416 *Vent.: ventilation, Fbiof: exchange with biofilm, SUR : surface runoff inputs, LAT : lateral inputs, GW :*  
 417 *groundwater inputs*

418

419 *Table 6: Simulated nitrogen in-stream processes on Toulouse-Malause section, interannual averages*  
 420 *(years 2000-2010), in tons per season and in percentage of total inputs (upstream, tributaries, point*  
 421 *sources, and diffuse inputs), in italics the highest value for each season.*

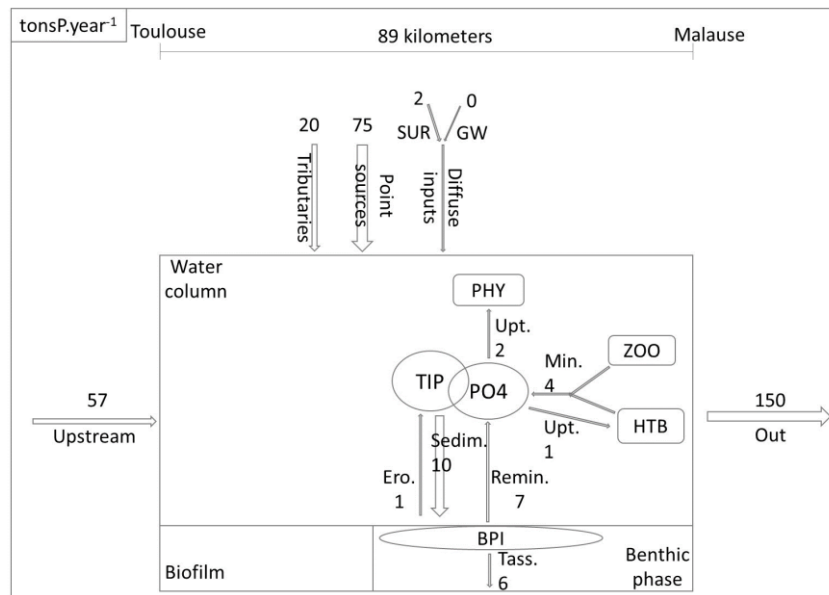
Variable	Process	Unit	Winter	Spring	Summer	Autumn	Year
NO <sub>3</sub> <sup>-</sup>	Flux across the water sediment interface	tonsN	-15.2	-16.0	-12.7	-22.1	-66.0
	Exchange with biofilm	tonsN	0	-0.1	-0.2	-0.6	-0.9
	Nitrataion	tonsN	2.2	1.4	2.4	7	13
	Phytoplankton uptake	tonsN	-0.1	-0.3	-0.2	-0.2	-0.8
	Water column denitrification	tonsN	0	0	0	0	0
	<b>Total</b>	<b>tonsN</b>	<b>-12.9</b>	<b>-15</b>	<b>-11</b>	<b>-15.8</b>	<b>-54.9</b>
	<b>Total inputs</b>	<b>%inputs</b>	<b>0.5</b>	<b>0.4</b>	<b>0.9</b>	<b>1.1</b>	<b>0.6</b>
NO <sub>2</sub> <sup>-</sup>	<b>Total inputs</b>	<b>tonsN</b>	<b>2350</b>	<b>3691</b>	<b>1183</b>	<b>1410</b>	<b>8634</b>
	Exchange with biofilm	tonsN	-0.2	-0.1	-0.1	-0.4	-0.8
	Ammonium oxidation	tonsN	-2.2	-1.4	-2.4	-7.0	-13.0
	Nitrite oxidation	tonsN	0.0	0.0	0.1	0.3	0.4
	<b>Total</b>	<b>tonsN</b>	<b>-2.3</b>	<b>-1.4</b>	<b>-2.4</b>	<b>-7.1</b>	<b>-13.2</b>
	<b>Total inputs</b>	<b>%inputs</b>	<b>2.2</b>	<b>3.9</b>	<b>18.5</b>	<b>8.8</b>	<b>5.6</b>
	<b>Total inputs</b>	<b>tonsN</b>	<b>106</b>	<b>36</b>	<b>13</b>	<b>81</b>	<b>236</b>
NH <sub>4</sub> <sup>+</sup>	Ammonification	tonsN	2.3	3.3	6.0	11.8	23.4
	Benthic remineralization	tonsN	6.2	6.3	0.5	-0.5	12.5
	Exchange with biofilm	tonsN	-0.1	-0.1	-0.2	-0.7	-1.1
	Heterotrophic bacteria uptake	tonsN	-0.6	-0.8	-1.7	-3.4	-6.5
	Nitrite oxidation	tonsN	0.0	0.0	-0.1	-0.3	-0.4
	Phytoplankton uptake	tonsN	-2.1	-4.1	-2.5	-4.6	-13.3
	<b>Total</b>	<b>tonsN</b>	<b>5.7</b>	<b>4.6</b>	<b>2</b>	<b>2.3</b>	<b>14.6</b>
<b>Total inputs</b>	<b>%inputs</b>	<b>2.9</b>	<b>2.3</b>	<b>1.6</b>	<b>0.9</b>	<b>1.9</b>	
N <sub>2</sub> O	<b>Total inputs</b>	<b>tonsN</b>	<b>195</b>	<b>196</b>	<b>126</b>	<b>253</b>	<b>770</b>
	Benthic denitrification	tonsN	0.9	0.9	0.9	1.7	4.4
	Nitrification	tonsN	0	0	0	0	0
	Ventilation	tonsN	-0.2	-0.2	-0.5	-1.1	-2.0
	<b>Total</b>	<b>tonsN</b>	<b>0.7</b>	<b>0.7</b>	<b>0.4</b>	<b>0.6</b>	<b>2.4</b>
	<b>Total inputs</b>	<b>%inputs</b>	<b>100</b>	<b>78</b>	<b>133</b>	<b>120</b>	<b>100</b>
	<b>Total inputs</b>	<b>tonsN</b>	<b>0.7</b>	<b>0.9</b>	<b>0.3</b>	<b>0.5</b>	<b>2.4</b>

422

### 423 3.2.2 Inorganic phosphorus budget

424 Urban effluents represented 40% of the section inputs, tributaries 11%, upstream 48%, and  
 425 diffuse inputs only 1% (Figure 8). According to Bonvallet Garay et al. (2001), Toulouse  
 426 sewage treatment plant represented between 59 and 67% of total phosphorus input in this  
 427 sector, before WWTPs treatment were upgraded in the 2000's.

428 2.4 tonsP.year<sup>-1</sup> (1.6% of the inputs) was removed from the water column along the section,  
 429 mainly with total inorganic phosphorus (TIP) sedimentation. Retention, and particularly  
 430 sedimentation, was higher in spring (Table 7). P retention was experimentally estimated on  
 431 the field at 22% of total phosphorus and 27% of dissolved reactive phosphorus on the first  
 432 half of this section in 1997 during low summer flows (Bonvallet Garay et al., 2001). Inorganic  
 433 phosphorus was also retained using Seneque-Riverstrahler applications on the Seine, Somme,  
 434 Scheldt rivers (Thieu et al., 2009), and on Red River (Le et al., 2010). In the former study, the  
 435 dominant processes were phytoplankton uptake, immobilization within the sediment, and  
 436 deposition (unspecified for the Red River study).



437

438 *Figure 8: Inorganic phosphorus budget on Toulouse-Malause section estimated with SWAT-RIVE model,*  
 439 *interannual averages, in tons of P per year, during the period 2000 to 2010. TIP: total inorganic*  
 440 *phosphorus, PO4: orthophosphates, BPI: benthic inorganic phosphorus, PHY: phytoplankton, HTB:*  
 441 *heterotrophic bacteria, ZOO: zooplankton, Upt.: phytoplankton or bacteria uptake, Min.: zooplankton and*  
 442 *heterotrophic bacteria mineralization, Ero.: BPI erosion, Sedim.: PIT sedimentation, Remin.: PO4 flux*  
 443 *associated with benthic remineralization, Tass.: compaction, SUR: surface runoff inputs, GW: groundwater*  
 444 *inputs.*

445

446 *Table 7: Simulated inorganic phosphorus in-stream processes on Toulouse-Malause section, interannual*  
 447 *averages (years 2000-2010), in tons per season and in percentage of total inputs (upstream, tributaries,*  
 448 *point sources, and diffuse inputs), in italics the highest value for each season.*

Variable	Process	Unit	Winter	Spring	Summer	Autumn	Year
TIP	Benthic remineralization	tonsP	1.6	1.7	1.1	2.2	6.6
	Erosion	tonsP	0.1	0.3	0.1	0.1	0.6
	Heterotrophic bacteria uptake	tonsP	-0.1	-0.1	-0.3	-0.6	-1.1
	Phytoplankton uptake	tonsP	-0.4	-0.8	-0.4	-0.8	-2.4
	Sedimentation	tonsP	-2.5	-3.6	-1.5	-2.5	-10.1
	Zooplankton and heterotrophic bacteria mineralization	tonsP	0.4	0.6	1	2	4
<b>Total</b>		<b>tonsP</b>	<b>-0.9</b>	<b>-1.9</b>	<b>0</b>	<b>0.4</b>	<b>-2.4</b>
		<b>%inputs</b>	<b>3.4</b>	<b>4.7</b>	<b>0</b>	<b>0.8</b>	<b>1.6</b>
<b>Total inputs</b>		<b>tonsP</b>	<b>37</b>	<b>41</b>	<b>26</b>	<b>49</b>	<b>153</b>

449

450

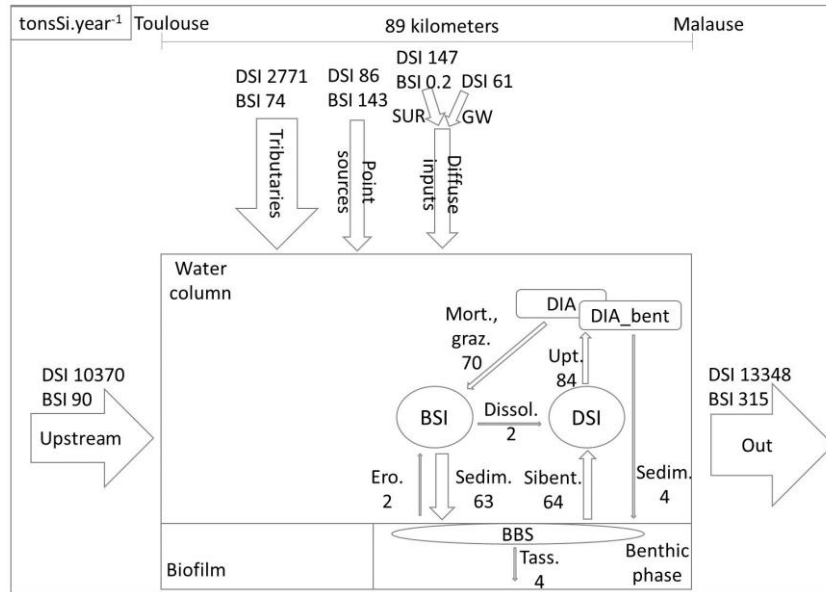
### 451 3.2.3 Silica budget

452 Dissolved silica (DSI) main inputs are upstream (77%) and tributaries (21%), biogenic silica  
 453 (BSI) are point sources (46%), upstream (29%), and tributaries (24%). Pyrenean floods  
 454 provide the majority of dissolved silica exported by the Garonne (Semhi et al., 2000).  
 455 Dissolved silica diffuse inputs were estimated with constant concentrations that varied  
 456 according to lithology, Future development should be made to estimate silica diffuse inputs  
 457 with SWAT model. Lechuga-Crespo et al. (2021) developed SWATLitho, which adds a

458 lithology layer and computes the major ion fluxes (excepted silica) reaching streams from  
459 chemical weathering of rocks. The average content of  $4.9 \text{ mgSi.gTSS}^{-1}$  applied for biogenic  
460 silica could be adapted with specific measurements in the modeled watershed. However, this  
461 value measured on the Seine watershed was also used by Liu et al. (2020) for modeling on the  
462 Rhine and Yangtze rivers (IMAGE-DGNM model, inspired by Riverstrahler) and Thieu et al.  
463 (2009) for the Riverstrahler modeling of the Somme and Scheldt rivers. Regarding point  
464 sources, biogenic silica loads are higher than dissolved silica. Conversely, Sferratore et al.  
465 (2006) measured dissolved silica loads almost twice as high as biogenic silica loads for  
466 Achères WWTP (Seine watershed). There were no available data on silica discharges for the  
467 Garonne watershed. Silica loads per inhabitant and treatment types used could be adapted  
468 with measurements.

469 DSI was consumed along the section ( $-19 \text{ tonsSi.year}^{-1}$ ). The dominant processes for DSI  
470 were a consumption by diatoms and drifted benthic diatoms, and a production by  
471 remineralization of DSI at the water-sediment interface (Figure 9). Net removal only  
472 represented 0.1% of the inputs: dissolved silica uptake by phytoplankton ( $84 \text{ tonsSi.year}^{-1}$ )  
473 was compensated by dissolved silica flux from the benthos ( $64 \text{ tonsSi.year}^{-1}$ ). Diatoms uptake  
474 was higher in spring and autumn. In summer, dissolved silica was not consumed but slightly  
475 produced (Table 8).  $8 \text{ tonsSi.year}^{-1}$  of biogenic silica (BSi) was formed (3% of the inputs)  
476 with the main production process being phytoplankton mortality and retention process  
477 through biogenic silica sedimentation. In winter, BSi retention logically exceeded production  
478 due to low biological activity. .

479 Muylaert et al. (2009) highlighted the negative correlation between measurements of  
480 dissolved silica and chlorophyll a concentrations downstream of Toulouse, suggesting the  
481 consumption of dissolved silica by diatoms. However, uptake and dissolution rates were not  
482 measured. Again, Seneque-Riverstrahler results also showed dissolved silica flux from  
483 benthic biogenic silica dissolution is not mentioned as dominant, unlike diatoms uptake and  
484 biogenic silica deposition (Thieu et al., 2009; Le et al., 2010). Nevertheless, the benthic  
485 algorithm used in this study is the new version (Billen et al., 2015). The low silica retention  
486 should also be related to the low simulated phytoplankton concentrations, compared to the  
487 observed ones, in the absence of water quality simulation for upstream reservoirs.



488  
489  
490  
491  
492  
493  
494

Figure 9: Silica budget on Toulouse-Malause section estimated with SWAT-RIVE model, interannual averages, in tons of Si per year, during the period 2000 to 2010. DSI: dissolved silica, BSI: biogenic silica, BBS: benthic biogenic silica, DIA: diatoms, DIA\_bent: drifted benthic diatoms, Upt.: diatoms and benthic diatoms uptake, Mort. Graz.: diatoms and benthic diatoms mortality or grazed, Dissol.: SIB dissolution, Sibent.: dissolved silica flux across the water-sediment interface, Sedim.: SIB or diatoms/benthic diatoms sedimentation, Ero.: BBS erosion, Tass.: compaction, SUR: surface runoff inputs, GW: groundwater inputs.

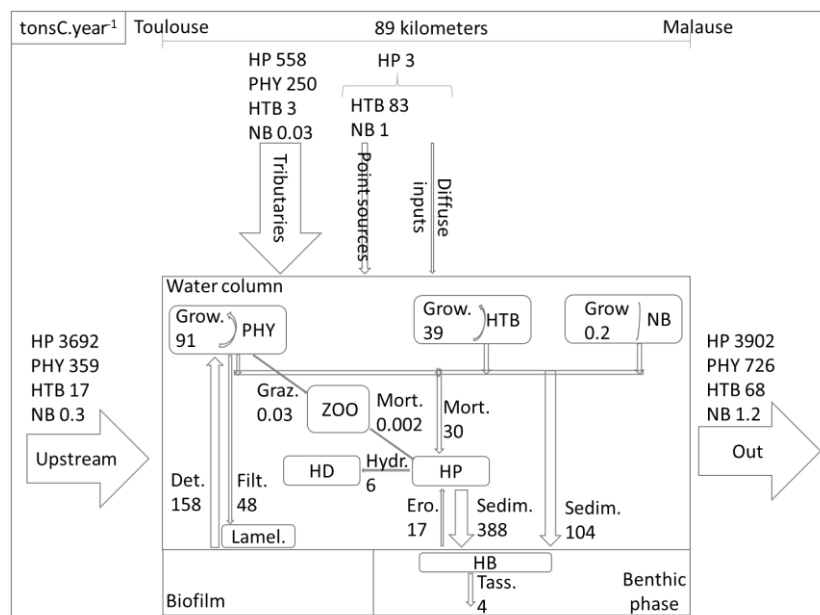
495 Table 8: Simulated silica in-stream processes on Toulouse-Malause section, interannual averages (years  
496 2000-2010), in tons per season and in percentage of total inputs (upstream, tributaries, point sources, and  
497 diffuse inputs), in *italics* the highest value for each season.

Variable	Process	Unit	Winter	Spring	Summer	Autumn	Year
DSi	Diatoms and drifted benthic diatoms uptake	tonsSi	-12.4	-26.4	-15.9	-29.5	-84.2
	Flux across the water-sediment interface	tonsSi	7.4	13.8	17.8	24.8	63.8
	SIB dissolution	tonsSi	0.2	0.3	0.5	0.8	1.8
	<b>Total</b>	<b>tonsSi</b>	<b>-4.8</b>	<b>-12.3</b>	<b>2.4</b>	<b>-3.9</b>	<b>-18.6</b>
	<b>Total inputs</b>	<b>tonsSi</b>	<b>3636</b>	<b>5877</b>	<b>1995</b>	<b>1858</b>	<b>13365</b>
BSi	Diatoms and drifted benthic diatoms mortality or grazed	tonsSi	10.5	19.5	14.3	26	70.3
	Dissolution	tonsSi	-0.2	-0.3	-0.5	-0.8	-1.8
	Erosion	tonsSi	0.4	1.5	0.3	0.2	2.4
	Sedimentation	tonsSi	-12.8	-17.7	-11.6	-20.6	62.7
	<b>Total</b>	<b>tonsSi</b>	<b>-2.1</b>	<b>3</b>	<b>2.5</b>	<b>4.8</b>	<b>8.2</b>
	<b>Total inputs</b>	<b>tonsSi</b>	<b>67</b>	<b>85</b>	<b>60</b>	<b>96</b>	<b>308</b>

498

499 **Organic suspended matter budget**

500 Organic suspended matter was represented in RIVE by several variables (phytoplankton,  
 501 nitrifying and heterotrophic bacteria and particulate non-living organic matter), described in  
 502  $\text{mgC.l}^{-1}$  (Figure 10). The in-stream processes resulted in the retention of heterotrophic bacteria  
 503 and particulate non-living organic matter through sedimentation. The input-output budget for  
 504 the phytoplankton species showed a production of biomass, with the drift of benthic diatoms  
 505 and their growth exceeding mortality, sedimentation, and lamellibranchs filtration.



506  
 507 *Figure 10: Organic suspended matter budget on Toulouse-Malause section estimated with SWAT-RIVE*  
 508 *model, interannual averages, in tons of C per year, during the period 2000 to 2010. PHY: phytoplankton,*  
 509 *HTB: heterotrophic bacteria, NB: nitrifying bacteria, ZOO: zooplankton, HP: particulate non-living*  
 510 *organic matter, HD: dissolved non-living organic matter, Grow.: growth, Mort.: mortality, Hydr.:*  
 511 *hydrolysis, Ero.: benthic organic matter erosion, Sedim.: sedimentation, Tass.: compaction, Det.: biofilm*  
 512 *algae detachment, Lamel.: lamellibranch, Filt.: lamellibranch filtration, Graz.: grazing.*

513  
 514 **3.3. Coupling SWAT and RIVE models: advantages**  
 515 **and difficulties**

516 To be in accordance with SWAT structure, RIVE equations replace QUAL2E equations, and  
 517 thus RIVE is applied on reach sections which have different length and residence time. SWAT  
 518 can be run in sub-daily time step; however, it would require sub-daily rainfall data, which  
 519 were not available.

520 Calculation time was similar for SWAT-RIVE and SWAT- QUAL2E models. With RIVE  
 521 model, the mass balance between the water column and the benthic zone is closed. No



522 numerical instabilities were noted, the numerical scheme applied was adequate for this  
523 watershed. However, Woldegiorgis et al. (2017)'s new quasi-analytical solution could be  
524 considered for further development, to compare the consistency and stability of SWAT-RIVE  
525 solutions.

526 Whereas SWAT hydrology and diffuse inputs need to be calibrated, an advantage of  
527 implementing the RIVE model was it does not require calibration, parameters being  
528 determined independently from the observations. However, some adjustments of the  
529 parameters can be made in the range of their experimental determination (e.g., Garnier et al.,  
530 2000; 2002). Minaudo et al. (2018) pointed out the need to calibrate such parameters as  
531 suspended sediment sedimentation velocity and the two parameters determining phosphorus  
532 adsorption. In this study, the particulate organic matter sinking rate was adjusted from 0.05  
533  $\text{m}\cdot\text{h}^{-1}$  to  $0.006 \text{ m}\cdot\text{h}^{-1}$ , as it appeared previously high considering the composition of particulate  
534 organic matter in the Garonne watershed, especially for slowly biodegradable matter, which is  
535 mainly composed of tree leaves reaching the water column.

536 Regarding validation, there was a lack of data concerning several variables of RIVE model, in  
537 particular zooplankton, heterotrophic bacteria, and nitrifying bacteria biomasses, so the  
538 simulated concentrations were not compared with such observations. Their correct  
539 representation is essential for the validity of the model, as they intervene in the  
540 biogeochemical cycles where variables are strongly interdependent (Minaudo et al., 2018).  
541 The parameters used in their representation do not justify calibration because they have been  
542 determined directly from experiments based on key physico-chemical parameters such as  
543 temperature dependency. However, measured data could be further used to validate the input  
544 settings, such as the estimations made for bacterial point sources.

545 The SWAT model version used in this study did not simulate silica and organic matter diffuse  
546 inputs, required by RIVE, so that alternative methods were applied for their input to the  
547 Garonne reach (discussed in section 3.2.3 for silica). DOC and POC concentrations were  
548 estimated at the beginning of each simulated day in every reach based on previously  
549 established relationships between DOC and discharge, and POC and TSS in the Garonne  
550 watershed (see Table 3). The DOC equation was validated on 58 watersheds out of 70 around  
551 the world (Fabre et al., 2020) and the POC one on the Save, a Garonne tributary, the Yenisei,  
552 the Mississippi, the Murray, the Oubangui and Hwang Ho (Boithias et al., 2014; Fabre et al.,  
553 2019; Fabre, 2019). Recent SWAT developments concerned the integration in SWAT of DOC  
554 and POC fluxes from land to river reaches (Du et al., 2019; Qi et al., 2020; Zhang et al.,

555 2013), but they were not integrated into the SWAT version available. On the other hand,  
556 while using RIVE, measurements of organic carbon biodegradability specific to the studied  
557 area would allow for a more precise refinement of the distribution within the biodegradability  
558 classes of the RIVE model.

## 559 **4. Conclusion**

560 The biogeochemical RIVE model was integrated into the river basin SWAT code. The  
561 coupled SWAT-RIVE model was successfully applied to a section of the Garonne in its  
562 middle course. We added a biofilm equation to accurately represent the algae communities in  
563 the river, dominated by drifted benthic diatoms. The simulated nutrients and oxygen  
564 concentrations and associated fluxes varied within the range of observed data, and the  
565 seasonal variations were adequately reproduced. The coupled model represents various  
566 additional variables, such as silica or phytoplankton major groups and it provides more  
567 information about the biological processes occurring in the drainage network compared to the  
568 previous version, including the removal of nitrate by benthic denitrification. Finally, it allows  
569 the user to avoid calibration for in-stream water quality parameters. Future improvements can  
570 be achieved by modifying and using SWAT model to calculate organic carbon and silica  
571 diffuse inputs from watersheds to streams, and by applying RIVE model not only to streams  
572 but also to reservoirs, which are major components of hydrosystems.

## 573 **Software availability**

- 574 • The Soil and Water Assessment Tool (SWAT) is freely available in  
575 <https://swat.tamu.edu/software/>. The version used is SWAT2012 VER 2016/Rev 664.
- 576 • RIVE is currently being revised and unified by the Metis Lab developers' team, to be  
577 open soon to the scientific community through a collaborative platform  
578 (<https://gitlab.in2p3.fr/rive>).
- 579 • Source code of the modified model presented in this paper (SWAT-RIVE) will be  
580 provided on the collaborative platform (<https://gitlab.in2p3.fr/rive>).

581

## 582 **Acknowledgments**

583 We would like to thank Electricité De France and the ANRT association (Association  
584 Nationale de la Recherche et de la Technologie) for their support, and members of Electricité  
585 De France (project REGARD-RTRA/STAE), Compagnie d'Aménagement des Coteaux de  
586 Gascogne and Banque Hydro that provide us data. Author contributions: S.M.:  
587 conceptualization, data curation, formal analysis, investigation, methodology, validation,  
588 visualization, software, writing - original draft, review & editing.; S.S.: conceptualization,  
589 methodology, validation, writing - review & editing, investigation, supervision, resources and  
590 project administration; R.S : conceptualization, methodology, validation, writing - review &  
591 editing, investigation, supervision, resources, funding acquisition and project administration;  
592 C.M.: conceptualization, methodology, validation, writing - review & editing, supervision,  
593 and project administration; J.G.: software, resources, writing - review & editing ; V.T.:  
594 software, resources, writing - review & editing; R.C.: data curation, resources, writing -  
595 review & editing ; J.M.S.P. conceptualization, methodology, validation, writing - review &  
596 editing, investigation, supervision, resources and project administration.

## 597 **References**

- 598 Améziane, T., Dauta, A., Le Cohu, R., 2003. Origin and transport of phytoplankton in a large river: The  
599 Garonne, France. *Archiv für Hydrobiologie* 156, 385–404. <https://doi.org/10.1127/0003-9136/2003/0156-0385>
- 601 Arnold, J.G., Srinivasan, R., Muttiah, R.S., Williams, J.R., 1998. Large Area Hydrologic Modeling and  
602 Assessment Part I: Model Development1. *JAWRA Journal of the American Water Resources*  
603 *Association* 34, 73–89. <https://doi.org/10.1111/j.1752-1688.1998.tb05961.x>
- 604 Billen, G., Garnier, J., Hanset, P., 1994. Modeling Phytoplankton Development in Whole Drainage  
605 Networks - the Riverstrahler Model Applied to the Seine River System. *Hydrobiologia* 289, 119–  
606 137. <https://doi.org/10.1007/BF00007414>
- 607 Billen, G., Garnier, J., Némery, J., Sebilo, M., Sferratore, A., Barles, S., Benoit, P., Benoît, M., 2007. A  
608 long-term view of nutrient transfers through the Seine river continuum. *Science of The Total*  
609 *Environment* 375, 80–97. <https://doi.org/10.1016/j.scitotenv.2006.12.005>
- 610 Billen, G., Garnier, J., Silvestre, M., 2015. A simplified algorithm for calculating benthic nutrient fluxes in  
611 river systems. *Ann. Limnol. - Int. J. Lim.* 51, 37–47. <https://doi.org/10.1051/limn/2014030>
- 612 Billen, G., Ramarson, A., Thieu, V., Théry, S., Silvestre, M., Pasquier, C., Hénault, C., Garnier, J., 2018.  
613 Nitrate retention at the river–watershed interface: a new conceptual modeling approach.  
614 *Biogeochemistry* 139, 31–51. <https://doi.org/10.1007/s10533-018-0455-9>
- 615 Boithias, L., Sauvage, S., Merlina, G., Jean, S., Probst, J.-L., Sánchez Pérez, J.M., 2014. New insight into  
616 pesticide partition coefficient  $K_d$  for modelling pesticide fluvial transport: Application to an  
617 agricultural catchment in south-western France. *Chemosphere* 99, 134–142.  
618 <https://doi.org/10.1016/j.chemosphere.2013.10.050>
- 619 Bonvallet Garay, S., Sauvage, S., Vervier, P., 2001. Hydromorphological control of phosphorus in a large  
620 free-flowing gravel bed river: the Garonne River (France). *Regul. Rivers: Res. Mgmt.* 17, 461–  
621 472. <https://doi.org/10.1002/rrr.662>
- 622 Boulêtreau, S., Garabétian, F., Sauvage, S., Sánchez- Pérez, J.-M., 2006. Assessing the importance of a  
623 self-generated detachment process in river biofilm models. *Freshwater Biology* 51, 901–912.  
624 <https://doi.org/10.1111/j.1365-2427.2006.01541.x>

625 Brion, N., Billen, G., 2000. Wastewater as a source of nitrifying bacteria in river systems: the case of the  
626 River Seine downstream from Paris. *Water Research* 34, 3213–3221.  
627 [https://doi.org/10.1016/S0043-1354\(00\)00075-0](https://doi.org/10.1016/S0043-1354(00)00075-0)

628 Brown, L.C., Barnwell, T.O., 1987. The enhanced stream water quality models QUAL2E and QUAL2E-  
629 UNCAS: documentation and user manual. US Environmental Protection Agency. Office of  
630 Research and Development.

631 Cakir, R., Sauvage, S., Gerino, M., Volk, M., Sánchez-Pérez, J.M., 2020. Assessment of ecological  
632 function indicators related to nitrate under multiple human stressors in a large watershed.  
633 *Ecological Indicators* 111, 106016. <https://doi.org/10.1016/j.ecolind.2019.106016>

634 Debele, B., Srinivasan, R., Parlange, J.-Y., 2008. Coupling upland watershed and downstream waterbody  
635 hydrodynamic and water quality models (SWAT and CE-QUAL-W2) for better water resources  
636 management in complex river basins. *Environ Model Assess* 13, 135–153.  
637 <https://doi.org/10.1007/s10666-006-9075-1>

638 Du, X., Zhang, X., Mukundan, R., Hoang, L., Owens, E.M., 2019. Integrating terrestrial and aquatic  
639 processes toward watershed scale modeling of dissolved organic carbon fluxes. *Environmental  
640 Pollution* 249, 125–135. <https://doi.org/10.1016/j.envpol.2019.03.014>

641 Eulin, A., Le Cohu, R., 1998. Epilithic diatom communities during the colonization of artificial substrates  
642 in the River Garonne (France). Comparison with the natural communities. *Archiv für  
643 Hydrobiologie* 79–106. <https://doi.org/10.1127/archiv-hydrobiol/143/1998/79>

644 Even, S., Poulin, M., Garnier, J., Billen, G., Servais, P., Chesterikoff, A., Coste, M., 1998. River ecosystem  
645 modelling: Application of the PROSE model to the Seine river (France), in: Amiard, J.-C., Le  
646 Rouzic, B., Berthet, B., Bertru, G. (Eds.), *Oceans, Rivers and Lakes: Energy and Substance  
647 Transfers at Interfaces*. Springer Netherlands, Dordrecht, pp. 27–45. [https://doi.org/10.1007/978-94-011-5266-2\\_3](https://doi.org/10.1007/978-94-011-5266-2_3)

648

649 Fabre, C., 2019. Rôle des zones humides alluviales dans la régulation des flux de nitrates et de carbone  
650 organique vers les eaux de surface à l'échelle des bassins versants (PhD Thesis). Toulouse, INPT.

651 Fabre, C., Sauvage, S., Probst, J.-L., Sánchez-Pérez, J.M., 2020. Global-scale daily riverine DOC fluxes  
652 from lands to the oceans with a generic model. *Global and Planetary Change* 194, 103294.  
653 <https://doi.org/10.1016/j.gloplacha.2020.103294>

654 Fabre, C., Sauvage, S., Tananaev, N., Noel, G.E., Teisserenc, R., Probst, J.L., Perez, J.M.S., 2019.  
655 Assessment of sediment and organic carbon exports into the Arctic ocean: The case of the Yenisei  
656 River basin. *Water Res.* 158, 118–135. <https://doi.org/10.1016/j.watres.2019.04.018>

657 Femeena, P.V., Chaubey, I., Aubeneau, A., McMillan, S.K., Wagner, P.D., Fohrer, N., 2020. An improved  
658 process-based representation of stream solute transport in the soil and water assessment tools.  
659 *Hydrological Processes* 34, 2599–2611. <https://doi.org/10.1002/hyp.13751>

660 Francesconi, W., Srinivasan, R., Pérez-Miñana, E., Willcock, S.P., Quintero, M., 2016. Using the Soil and  
661 Water Assessment Tool (SWAT) to model ecosystem services: A systematic review. *Journal of  
662 Hydrology* 535, 625–636. <https://doi.org/10.1016/j.jhydrol.2016.01.034>

663 Garnier, J., Billen, G., Coste, M., 1995. Seasonal succession of diatoms and Chlorophyceae in the drainage  
664 network of the Seine River: Observation and modeling. *Limnology and Oceanography* 40, 750–  
665 765. <https://doi.org/10.4319/lo.1995.40.4.0750>

666 Garnier, J., Billen, G., Hannon, E., Fonbonne, S., Videnina, Y., Soulie, M., 2002. Modelling the Transfer  
667 and Retention of Nutrients in the Drainage Network of the Danube River. *Estuarine, Coastal and  
668 Shelf Science* 54, 285–308. <https://doi.org/10.1006/ecss.2000.0648>

669 Garnier, J., Billen, G., Sanchez, N., Leporcq, B., 2000. Ecological functioning of the Marne reservoir  
670 (upper Seine basin, France). *Regulated Rivers: Research & Management* 16, 51–71.  
671 [https://doi.org/10.1002/\(SICI\)1099-1646\(200001/02\)16:1<51::AID-RRR571>3.0.CO;2-I](https://doi.org/10.1002/(SICI)1099-1646(200001/02)16:1<51::AID-RRR571>3.0.CO;2-I)

672 Garnier, J., Ramarson, A., Billen, G., Thery, S., Thiery, D., Thieu, V., Minaudo, C., Moatar, F., 2018a.  
673 Nutrient inputs and hydrology together determine biogeochemical status of the Loire River  
674 (France) : Current situation and possible future scenarios. *Science of the Total Environment* 637,  
675 609–624. doi :10.1016/j.scitotenv.2018.05.045. place : AmsterdamPublisher : Elsevier Science Bv  
676 WOS :000436605400059.

677 Garnier, J., Ramarson, A., Thieu, V., Némery, J., Théry, S., Billen, G., Coynel, A., 2018b. How can water  
678 quality be improved when the urban waste water directive has been fulfilled? A case study of the  
679 Lot river (France). *Environmental Science and Pollution Research* 25.  
680 <https://doi.org/10.1007/s11356-018-1428-1>

- 681 Gassman, P.W., Reyes, M.R., Green, C.H., Arnold, J.G., 2007. The soil and water assessment tool:  
682 Historical development, applications, and future research directions. *Trans. ASABE* 50, 1211–  
683 1250.
- 684 Gassman, P.W., Sadeghi, A.M., Srinivasan, R., 2014. Applications of the SWAT Model Special Section:  
685 Overview and Insights. *J Environ Qual* 43, 1–8. <https://doi.org/10.2134/jeq2013.11.0466>
- 686 Grunwald, S., Qi, C., 2006. Gis-Based Water Quality Modeling in the Sandusky Watershed, Ohio, Usa1.  
687 *JAWRA Journal of the American Water Resources Association* 42, 957–973.  
688 <https://doi.org/10.1111/j.1752-1688.2006.tb04507.x>
- 689 Houser, J., Hauck, L., 2002. Analysis of the In-stream Water Quality Component of SWAT (Soil Water  
690 Assessment Tool), in: *Total Maximum Daily Load (TMDL): Environmental Regulations,*  
691 *Proceedings of 2002 Conference. American Society of Agricultural and Biological Engineers*, p.  
692 52.
- 693 Kim, N., Shin, A., 2011. Modification of the Channel BOD Simulation Scheme in SWAT for Korean  
694 TMDL Application. *Transactions of the ASABE* 54, 1739–1747.  
695 <https://doi.org/10.13031/2013.39839>
- 696 Kling, H., Fuchs, M., Paulin, M., 2012. Runoff conditions in the upper Danube basin under an ensemble of  
697 climate change scenarios. *Journal of Hydrology* 424–425, 264–277.  
698 <https://doi.org/10.1016/j.jhydrol.2012.01.011>
- 699 Krysanova, V., Arnold, J.G., 2008. Advances in ecohydrological modelling with SWAT—a review.  
700 *Hydrological Sciences Journal* 53, 939–947. <https://doi.org/10.1623/hysj.53.5.939>
- 701 Krysanova, V., White, M., 2015. Advances in water resources assessment with SWAT—an overview.  
702 *Hydrological Sciences Journal* 60, 771–783. <https://doi.org/10.1080/02626667.2015.1029482>
- 703 Le, T.P.Q., Billen, G., Garnier, J., Théry, S., Ruelland, D., Anh, N., Minh, C., 2010. Nutrient (N, P, Si)  
704 transfers in the subtropical Red River system (China and Vietnam): Modelling and budget of  
705 nutrient sources and sinks. *Journal of Asian Earth Sciences* 37.  
706 <https://doi.org/10.1016/j.jseaes.2009.08.010>
- 707 Lechuga-Crespo, J.L., Sauvage, S., Ruiz-Romera, E., George, C., Sánchez-Pérez, J.M., 2021. SWATLitho:  
708 A hydrogeochemical model to estimate daily geochemical loads at the catchment scale.  
709 *Environmental Modelling & Software* 135, 104893. <https://doi.org/10.1016/j.envsoft.2020.104893>
- 710 Liu, X., Joost van Hoek, W., Vilmin, L., Beusen, A., Mogollón, J.M., Middelburg, J.J., Bouwman, A.F.,  
711 2020. Exploring Long-Term Changes in Silicon Biogeochemistry Along the River Continuum of  
712 the Rhine and Yangtze (Changjiang). *Environ. Sci. Technol.* 54, 11940–11950.  
713 <https://doi.org/10.1021/acs.est.0c01465>
- 714 Maavara, T., Dürr, H.H., Van Cappellen, P., 2014. Worldwide retention of nutrient silicon by river  
715 damming: From sparse data set to global estimate. *Global Biogeochemical Cycles* 28, 842–855.  
716 <https://doi.org/10.1002/2014GB004875>
- 717 Migliaccio, K.W., Chaubey, I., Haggard, B.E., 2007. Evaluation of landscape and instream modeling to  
718 predict watershed nutrient yields. *Environmental Modelling & Software* 22, 987–999.  
719 <https://doi.org/10.1016/j.envsoft.2006.06.010>
- 720 Meybeck, M., 1986. Composition chimique des ruisseaux non pollués en France. Chemical composition of  
721 headwater streams in France. *Sciences Géologiques, bulletins et mémoires* 39, 3–77.  
722 <https://doi.org/10.3406/sgeol.1986.1719>
- 723 Minaudo, C., Curie, F., Jullian, Y., Gassama, N., Moatar, F., 2018. QUAL-NET, a high temporal-resolution  
724 eutrophication model for large hydrographic networks. *Biogeosciences* 15, 2251–2269.  
725 <https://doi.org/10.5194/bg-15-2251-2018>
- 726 Moriasi, D., Gitau, M., Pai, N., Daggupati, P., 2015. Hydrologic and Water Quality Models: Performance  
727 Measures and Evaluation Criteria. *Transactions of the ASABE (American Society of Agricultural*  
728 *and Biological Engineers)* 58, 1763–1785. <https://doi.org/10.13031/trans.58.10715>
- 729 Muylaert, K., Sanchez-Pérez, J.M., Teissier, S., Sauvage, S., Dauta, A., Vervier, P., 2009. Eutrophication  
730 and its effect on dissolved Si concentrations in the Garonne River (France). *J Limnol* 68, 368.  
731 <https://doi.org/10.4081/jlimnol.2009.368>
- 732 Narasimhan, B., Srinivasan, R., Bednarz, S.T., Ernst, M., Allen, P., 2010. A Comprehensive Modeling  
733 Approach for Reservoir Water Quality Assessment and Management Due to Point and Nonpoint  
734 Source Pollution. *Transactions of the ASABE* 53. <https://doi.org/10.13031/2013.34908>
- 735 Neitsch, S.L., Arnold, J.G., Kiniry, J.R., Williams, J.R., 2011. Soil and water assessment tool theoretical  
736 documentation version 2009. Texas Water Resources Institute.
- 737 Noh, J., Kim, J.-C., Park, J., 2013. Turbidity control in downstream of the reservoir: The Nakdong River in  
738 Korea. *Environmental Earth Sciences* 71. <https://doi.org/10.1007/s12665-013-2589-3>

739 Oeurng, C., Sauvage, S., Sanchez-Perez, J.-M., 2011. Assessment of hydrology, sediment and particulate  
740 organic carbon yield in a large agricultural catchment using the SWAT model. *J. Hydrol.* 401,  
741 145–153. <https://doi.org/10.1016/j.jhydrol.2011.02.017>

742 Pinay, G., Ruffinoni, C., Wondzell, S., Gazelle, F., 1998. Change in Groundwater Nitrate Concentration in  
743 a Large River Floodplain: Denitrification, Uptake, or Mixing? *Journal of the North American*  
744 *Benthological Society* 17, 179–189. <https://doi.org/10.2307/1467961>

745 Pyo, J., Pachepsky, Y.A., Kim, M., Baek, S.-S., Lee, H., Cha, Y., Park, Y., Cho, K.H., 2019. Simulating  
746 seasonal variability of phytoplankton in stream water using the modified SWAT model.  
747 *Environmental Modelling & Software* 122, 104073. <https://doi.org/10.1016/j.envsoft.2017.11.005>

748 Qi, J., Du, X., Zhang, X., Lee, S., Wu, Y., Deng, J., Moglen, G.E., Sadeghi, A.M., McCarty, G.W., 2020.  
749 Modeling riverine dissolved and particulate organic carbon fluxes from two small watersheds in  
750 the northeastern United States. *Environmental Modelling & Software* 124, 104601.  
751 <https://doi.org/10.1016/j.envsoft.2019.104601>

752 Ruelland, D., Billen, G., Brunstein, D., Garnier, J., 2007a. SENEQUE: A multi-scaling GIS interface to the  
753 Riverstrahler model of the biogeochemical functioning of river systems. *Science of The Total*  
754 *Environment, Human activity and material fluxes in a regional river basin: the Seine River*  
755 *watershed* 375, 257–273. <https://doi.org/10.1016/j.scitotenv.2006.12.014>

756 Ruelland, D., Silvestre, M., Thieu, V., Billen, G., 2007b. Applicatif SENEQUE 3.4: notice d'utilisation.  
757 PIREN-Seine: Paris, France.

758 Sánchez-Pérez, J.M., Vervier, P., Garabétian, F., Sauvage, S., Loubet, M., Rols, J.L., Bariac, T., Weng, P.,  
759 2003. Nitrogen dynamics in the shallow groundwater of a riparian wetland zone of the Garonne,  
760 SW France: nitrate inputs, bacterial densities, organic matter supply and denitrification  
761 measurements. *Hydrology and Earth System Sciences Discussions* 7, 97–107.

762 Semhi, K., Amiotte Suchet, P., Clauer, N., Probst, J.-L., 2000. Dissolved silica in the Garonne River  
763 waters: changes in the weathering dynamics. *Environmental Geology* 40, 19–26.  
764 <https://doi.org/10.1007/s002540000119>

765 Sferratore, A., Billen, G., Garnier, J., Smedberg, E., Humborg, C., Rahm, L., 2008. Modelling nutrient  
766 fluxes from sub-arctic basins: Comparison of pristine vs. dammed rivers. *Journal of Marine*  
767 *Systems, Silicon and the Baltic Sea* 73, 236–249. <https://doi.org/10.1016/j.jmarsys.2007.10.012>

768 Sferratore, A., Garnier, J., Billen, G., Conley, D.J., Pinault, S., 2006. Diffuse and Point Sources of Silica in  
769 the Seine River Watershed. *Environ. Sci. Technol.* 40, 6630–6635.  
770 <https://doi.org/10.1021/es060710q>

771 Simeoni-Sauvage, S., 1999. Modélisation hydrobiogéochimique de la Garonne à l'étiage estival : cas de  
772 l'azote entre Toulouse et Agen (120 kilomètres) (These de doctorat). Toulouse, INPT.

773 Sow, M.M., Majdi, N., Muylaert, K., Tackx, M., Julien, F., Probst, J.-L., Mialet, B., Sutra, C., Probst, A.,  
774 Thébault, J.-M., Kenarlikdjian, M., Gérino, M., 2016. Retention of nutrients, suspended particulate  
775 matter and phytoplankton in a pondage associated with a run-of-the-river type hydroelectric power  
776 plant. *Ecohydrology* 9, 229–237. <https://doi.org/10.1002/eco.1626>

777 Sun, X., Bernard-Jannin, L., Garneau, C., Volk, M., Arnold, J.G., Srinivasan, R., Sauvage, S., Sanchez-  
778 Perez, J.M., 2016. Improved simulation of river water and groundwater exchange in an alluvial  
779 plain using the SWAT model. *Hydrol. Process.* 30, 187–202. <https://doi.org/10.1002/hyp.10575>

780 Sun, X., Bernard-Jannin, L., Grusson, Y., Sauvage, S., Arnold, J., Srinivasan, R., Perez, J.M.S., 2018.  
781 Using SWAT-LUD Model to Estimate the Influence of Water Exchange and Shallow Aquifer  
782 Denitrification on Water and Nitrate Flux. *Water* 10, 528. <https://doi.org/10.3390/w10040528>

783 Teissier, S., Torre, M., Delmas, F., Garabétian, F., 2007. Detailing biogeochemical N budgets in riverine  
784 epilithic biofilms. *Journal of the North American Benthological Society* 26, 178–190.  
785 [https://doi.org/10.1899/0887-3593\(2007\)26\[178:dbnbir\]2.0.co;2](https://doi.org/10.1899/0887-3593(2007)26[178:dbnbir]2.0.co;2)

786 Tekwani, N., Majdi, N., Mialet, B., Tornès, E., Urrea-Clos, G., Buffan-Dubau, E., Sabater, S., Tackx, M.,  
787 2013. Contribution of epilithic diatoms to benthic–pelagic coupling in a temperate river. *Aquatic*  
788 *Microbial Ecology* 69, 47–57. <https://doi.org/10.3354/ame01616>

789 Thieu, V., Billen, G., Garnier, J., 2009. Nutrient transfer in three contrasting NW European watersheds:  
790 The Seine, Somme, and Scheldt Rivers. A comparative application of the Seneque/Riverstrahler  
791 model. *Water Research* 43, 1740–1754. <https://doi.org/10.1016/j.watres.2009.01.014>

792 Thieu V., Silvestre M., Casquin A., Garnier J., Billen G., 2022. Modelling of carbon and nutrient transfers  
793 in French rivers: First step of a national generic land to sea modelling chain to fight against coastal  
794 eutrophication. 4th Int. Conf. Integr. Sci. Sustain. Dev. Rivers. 4-8 july, Lyon-France.

795 Uehlinger, U., Bühner, H., Reichert, P., 1996. Periphyton dynamics in a floodprone prealpine river:  
796 evaluation of significant processes by modelling. *Freshwater Biology* 36, 249–263.  
797 <https://doi.org/10.1046/j.1365-2427.1996.00082.x>

798 Van Griensven, A., Bauwens, W., 2003. River water quality management for the Senne river Basin  
799 (Belgium). *Eur Water* 1, 9–15.

800 Vilmin, L., Aissa-Grouz, N., Garnier, J., Billen, G., Mouchel, J.-M., Poulin, M., Flipo, N., 2015. Impact of  
801 hydro-sedimentary processes on the dynamics of soluble reactive phosphorus in the Seine River.  
802 *Biogeochemistry* 122, 229–251. <https://doi.org/10.1007/s10533-014-0038-3>

803 White, M.J., Storm, D.E., Mittelstet, A., Busteed, P.R., Haggard, B.E., Rossi, C., 2014. Development and  
804 Testing of an In-Stream Phosphorus Cycling Model for the Soil and Water Assessment Tool.  
805 *Journal of Environmental Quality* 43, 215–223. <https://doi.org/10.2134/jeq2011.0348>

806 Woldegiorgis, B.T., van Griensven, A., Pereira, F., Bauwens, W., 2017. A new unconditionally stable and  
807 consistent quasi-analytical in-stream water quality solution scheme for CSTR-based water quality  
808 simulators. *Water Resources Research* 53, 4668–4690. <https://doi.org/10.1002/2016WR019558>

809 X., Zhang, S., Li, S., Zhang, Liwei, Wang, G., Zhang, Ling, Wang, J., Li, Z., 2018. The cycle of  
810 nitrogen in river systems: sources, transformation, and flux. *Environ. Sci. Process. Impacts* 20,  
811 863–891. <https://doi.org/10.1039/C8EM00042E>

812 Yan, X., Thieu, V., Garnier, J., 2021. Long-term assessment of nutrient budgets for the four reservoirs of  
813 the Seine Basin (France). *Science of The Total Environment* 778, 146412.  
814 <https://doi.org/10.1016/j.scitotenv.2021.146412>

815 Zhang, X., Izaurralde, R.C., Arnold, J.G., Williams, J.R., Srinivasan, R., 2013. Modifying the Soil and  
816 Water Assessment Tool to simulate cropland carbon flux : Model development and initial  
817 evaluation. *Science of The Total Environment* 463-464, 810–822. URL :  
818 <http://www.sciencedirect.com/science/article/pii/S0048969713007080>, doi  
819 :10.1016/j.scitotenv.2013.06.056.